Food Chemistry 210 (2016) 388–395

Contents lists available at ScienceDirect

Food Chemistry

journal homepage: www.elsevier.com/locate/foodchem

Dynamic high pressure microfluidization treatment of zein in aqueous ethanol solution

Cuixia Sun, Lei Dai, Fuguo Liu, Yanxiang Gao *

Beijing Advanced Innovation Center for Food Nutrition and Human Health, Beijing Laboratory for Food Quality and Safety, Beijing Key Laboratory of Functional Food from Plant Resources, College of Food Science & Nutritional Engineering, China Agricultural University, 100083, China

ARTICLE INFO

Article history:
Received 23 January 2016
Received in revised form 26 April 2016
Accepted 30 April 2016
Available online 30 April 2016

Keywords:
Zein
DHPM treatment
Thermal behaviors
Structure
Morphology

ABSTRACT

Dynamic high pressure microfluidization (DHPM) treatment at the pressures of 25, 50, 75, 100, 125 and 150 MPa was performed to explore its effects on the characteristics of zein in aqueous ethanol solution. The results showed that after DHPM treatment at 125 MPa, the volume percentage of zein nanoparticles ($d < 100$ nm) was increased from 68.8% to 94.7%, and the fluorescence intensity approached to the maximum. DHPM treatment at the pressure of 25 MPa led to the increase of α-helix and β-sheet of zein from 57.1% to 59.4% and from 16.8% to 17.9%, respectively. The partial denaturation of zein was induced after DHPM process at pressures from 50 to 150 MPa. The morphology of zein was modified from nanosphere to the needle-like shapes after DHPM treatment at 75 MPa, and the deduction was proposed that the morphological change at 75 MPa was ascribed to the existence of the intermediate transition state.

1. Introduction

Zein, a plant protein from corn, belongs to the class of prolamins and is regarded as a valuable food ingredient with many advantages such as environment-friendly, biodegradable, non-toxic, edible, and broad application prospects (Paliwal & Palakurthi, 2014). Being the amphiphilic protein, zein can form spherical colloidal nanoparticles which are often applied for controlled and targeted delivery of bioactive compounds in food, pharmaceutical and biotechnological industries (Patel & Velikov, 2014).

Zein shows the inherent hydrophobicity due to the high proportion of non-polar amino acid residues, which makes up more than 50% of its total amino acid content (Lawton, 2002). As a result, zein is insoluble in water but easily soluble in aqueous ethanol, and its solubility is dependent on the concentration of alcohol. There are two liquid phases at lower (<40%) and higher (>90%) concentrations of ethanol (Osborne, 1897). According to the report of Argos, Pedersen, Marks, and Larkins (1982), zein had a helical wheel structure with nine homologous repeating units arranged in an anti-parallel form stabilized by hydrogen bonds. The result of small-angle X-ray scattering measurement showed that zein exhibited an elongated molecular structure (Matsushima, Danno, Takezawa, & Izumi, 1997). Yamada, Noguchi, and Takhashi (1996) reported that zein in aqueous ethanol solution formed aggregates containing small globules. Circular dichroism measurement revealed that the α-helical content of zein varied between 33.6% and 60% in 50%–80% aqueous ethanol solution (Cabra, Arreguin, Vazquez-Duhalt, & Farres, 2006).

It is well known that structures of proteins determine their properties. The modification of zein is required to broaden its application. Previous studies reported the acidic or alkaline deamidation or enzymatic hydrolysis (Funatsu & Shibata, 1998) to modify the functional properties of zein. Nowadays, the new trend of protein modifications focus on application of physical treatments such as high pressure homogenization, static ultra high pressure and dynamic high pressure microfluidization (DHPM), which can modify most globular protein by affecting hydrogen and hydrophobic interactions.

DHPM, a novel mean of homogenization technology, consists of two types of process chambers including Y-type and Z-type. The combination of Y and Z-type chambers is often used to prepare nano/micro-emulsion, while the series connection between two Z-type chambers is commonly applied to broke droplets (Cook & Lagace, 1987). DHPM shows the combined forces of cavitation, shear, high-velocity impact and has gained a popular application in pharmaceutical and cosmetic industries, as well as food processing for milk homogenization to extend its shelf life (Pereda, Ferragut, Quevedo, Guamis, & Trujillo, 2008). Previous studies of DHPM focused on the production of liposomes (Lajunen et al., 2014), and the modification of physiochemical, functional and structural properties for water soluble proteins (Shen & Tang, 2012). However, little information is available about the effect of DHPM on structural modifications of alcohol-soluble proteins.

* Corresponding author.
E-mail address: gyxcau@126.com (Y. Gao).

http://dx.doi.org/10.1016/j.foodchem.2016.04.138
0308-8146/

The objective of present study was to explore the effect of DHPM treatment on the physical, structural, thermal and morphological characteristics of zein in ethanol-water solution. Results from present work can be used to confirm the hypothesis that the DHPM treatment would be an attractive modification method for zein with better thermal behaviors and structural properties to develop a new food ingredient, which could play an important role in establishing the potential delivery systems for bioactive compounds.

2. Materials and methods

2.1. Materials

Zein with a protein content of 95% (w/w) was purchased from Gaoyou Group Co. Ltd. (Jiangsu, China). Absolute ethanol (99.9%) was acquired from Eshowbokoo Biological Technology Co., Ltd. (Beijing, China). Water purified by a MilliQ system (Millipore, MA, USA) was used for all the experiments.

2.2. DHPM treatment of zein in aqueous ethanol solution

DHPM treatment of zein solution was performed with the method of Chen, Gao, Yang, and Gao (2013) with some modifications. Stock zein solution (1%, w/v) was prepared by dissolving the native zein in aqueous ethanol solution (70% v/v), then the solution was subjected to the treatment at a specific pressure of 25, 50, 75, 100, 125 and 150 MPa using a Microfluidizer® processor model M-110EH (Microfluidics, Newton, MA, USA). The machine was equipped with two ceramic chambers: interaction chamber IXC type H30Z (entry point diameter 200 μm). All the samples passed through the system two times, the treated samples were stored at 5 °C prior to the further analysis. The replication for the DHPM treatment at the individual batches of pressures from 25 to 150 MPa was made for three times.

In this work, samples of untreated and DHPM-treated zein in ethanol-water solution at different processing pressures of 25, 50, 75, 100, 125 and 150 MPa were termed as Zein, Zein-DHPM$_{25}$, Zein-DHPM$_{50}$, Zein-DHPM$_{75}$, Zein-DHPM$_{100}$, Zein-DHPM$_{125}$ and Zein-DHPM$_{150,}$ respectively.

2.3. Preparation of zein colloidal nanoparticles

Zein colloidal nanoparticles were prepared by the anti-solvent precipitation method adapted from Luo, Teng, Wang, and Wang (2013). Briefly, 60 mL deionized water was put into a beaker and stirred vigorously. DHPM-treated zein solution (20 mL) was added in 2 min to this beaker using a syringe with a plunger speed of 10 mL/min. To acquire aqueous dispersions, approximately three quarters of ethanol were distilled to remove under reduced pressure by rotary evaporation at 45 °C for 20 min. Finally, zein colloidal dispersions at around 4.0 were stored in the refrigerator at 5 °C for further analysis in a liquid form, and part of the dispersions were freeze-dried for 48 h to acquire dry particles for solid state characterization analysis. Zein colloidal dispersions without DHPM treatment were obtained by the aforementioned process and used as the control sample.

2.4. Determination of particle size distribution

Particle size distribution was determined by dynamic light scattering (DLS) using a Zetasizer Nano-ZS90 (Malvern Instruments Ltd., Worcestershire, UK) on the base of the description of Wang et al. (2015) with slight modifications. Freshly prepared native and DHPM-treated zein colloidal dispersions were diluted by 5 times with MilliQ water at room temperature before measurements to avoid multiple particle effects. The refractive index of the globule protein and the dispersant (water) at 25 °C was 1.456 and 1.330, respectively. The measurements were made using a quartz cuvette with a path length of 1 cm. All measurements were carried out at room temperature (25 °C) and each sample was analyzed in triplicate.

2.5. Turbidity measurement

The turbidity of native and DHPM-treated zein colloidal dispersions was evaluated by a HACH 2100N laboratory turbidimeter (Loveland, USA). The optical apparatus was equipped with a tungsten-filament lamp with three detectors: a 90° scattered-light detector, a forward-scatter light detector, and a transmitted light detector. The calibration was performed using a Gelex Secondary Turbidity Standard Kit (HACH, Loveland, USA), which consists of stable suspensions of a metal oxide in a gel. All experiments were performed in triplicate.

2.6. Fluorescence analysis

Fluorescence measurement was performed by a fluorescence spectrophotometer (F-7000, Hitachi, Japan) according to the method of our previous study (Sun et al., 2015). Scanning parameters were optimized with the slit width of 20 nm for excitation and 10 nm for emission. The excitation wavelength was set at 280 nm to selectively excite the tryptophan residues, and the emission spectra were collected between 290 and 450 nm with a scanning speed of 100 nm/min. Both excitation and emission slit widths were set at 10 nm. Each individual emission spectrum was the average result of three runs and all data were collected at room temperature.

2.7. Ultraviolet spectroscopic analysis

The ultraviolet absorption spectra of zein colloidal dispersions were determined after an appropriate dilution by using UV-1800 spectrophotometer (Shimadzu Corporation, Kyoto, Japan). The scanning range was 200–450 nm at a medium speed of 200 nm/min.

2.8. Circular dichroism spectra

Far-UV CD spectra of the samples were recorded in the range of 190–260 nm by a CD spectrometer (Pistar π-180, Applied Photophysics Ltd. UK). During the process of data collection, the protein concentration was 0.2 mg/mL, a quartz cell with a 1 mm path length was selected, a constant nitrogen flush was applied, and ellipticity was recorded at a speed of 100 nm/min, 0.2 nm resolution, 20 accumulations and 2.0 nm bandwidth. The secondary structure contents of the samples were estimated using Dichroweb: Circular Dichroism Website http://dichroweb.cryst.bbk.ac.uk (Lobley, Whitmore, & Wallace, 2002).

2.9. Differential scanning calorimetry (DSC) analysis

The calorimetric analyses of the freeze-dried samples were performed by a DSC-60 thermal analysis system (Shimadzu, Tokyo, Japan) in the light of the description of Mizutani, Matsumura, Murakami, and Mori (2004) with some modifications. In a standard procedure, 3.0 mg samples were placed inside an aluminum pan and sealed tightly by a perforated aluminum lid, and heating schedule was set from 30 to 320 °C at a constant rate of 10 °C/min with an invariable purging of dry nitrogen at a constant rate of 30 mL/min. An empty aluminum pan was used as a control. The denatured and melting temperatures were computed using the universal analysis software from each thermal curve.

2.10. Transmission electron microscopy analysis

According to the introduced method of Patel, Bouwens, and Velikov (2010), the particle morphology was analyzed by transmission electron microscopy (TEM) using Tecnai 200 transmission electron microscope (FEI Company, The Netherlands) at an accelerating voltage of 60 kV (Philips, NL-5600 MD, Eindhoven, the Netherlands). The particles were dispersed in aqueous ethanol solution (70% v/v) and one drop of the diluted dispersion was placed on a 200-mesh carbon coated copper grid.

2.11. Statistical analysis

All the collected data were the average values of triplicate determinations and the results were expressed as mean value ± standard deviation (SD) in this study. Data were subjected to statistical analysis of variance (ANOVA) using the software package SPSS 18.0 for Windows (SPSS Inc., Chicago, USA). Least significant differences ($p < 0.05$) were accepted using the Duncan procedure.

3. Results and discussion

3.1. Particle size distribution and turbidity

The effects of DHPM treatment at different pressures on particle size distribution in volume percentage, average size and turbidity of zein colloidal dispersions are shown in Fig. 1A and B, respectively. Typical monomodal particle size distribution curves were observed for all samples in Fig. 1A. The distribution of the native zein nanoparticles was wide. However, the DHPM-treated zein nanoparticles exhibited the sharp peak. The volume percentage of small particles (d < 100 nm) in native zein colloidal dispersion was 68.8%, which was significantly ($p < 0.05$) increased to 90.3%, 92.5%, 94.7% and 87.5% after DHPM treatment at the pressures of 25, 75, 125 and 150 MPa, respectively, indicating a narrower particle size distribution after DHPM treatment. It has been demonstrated that a decrease in fat globule size of bovine milk was found after ultra high pressure homogenization treatment (Hayes, Fox, & Kelly, 2005). Arzeni et al. (2012) found that ultrasound treatment resulted in a significant reduction in protein aggregate size for soy protein isolate. In the present work, the treatment at the pressure of 125 MPa gave the narrowest range in the size distribution of zein nanoparticles. Ciron, Gee, Kelly, and Auty (2010) reported that the milk microfluidized at 150 MPa had smaller particle size with narrower distribution. The resulting difference might be attributed to the diverse protein structures with variant properties. On the contrary, compared with the magnitude of the applied pressures, zein nanoparticles treated at 50 and 100 MPa presented the wider particle size distributions, indicating that some extent coalescence phenomenon could take place under these DHPM-treated pressures.

Nephelometry was performed to obtain some information about the effect of DHPM treatment on the turbidity change of samples. As shown in Fig. 1B, the turbidity of native zein colloidal dispersion was 746 NTU, which was significantly ($p < 0.05$) decreased to 372, 575, 623 and 675 NTU after DHPM treatment at the pressures of 25, 75, 125 and 150 MPa, respectively. Oppositely, the turbidity was greatly ($p < 0.05$) increased to 889 and 1287 NTU when the pressure reached to 50 and 100 MPa, respectively. The change of turbidity could be also directly perceived as illustrated in Fig. 1B.

The decreased turbidity suggested the formation of zein nanoparticles with more compact structure, which could be confirmed by the smaller particle size after the DHPM treatment in a certain pressure range as shown in Fig. 1A. Similarly, the increased turbidity might be attributed to the fact that large zein nanoparticles were generated due to their aggregation when the treated pressures were 50 and 100 MPa, which could also be interpreted by the wider size distribution under these pressures as presented in Fig. 1A.

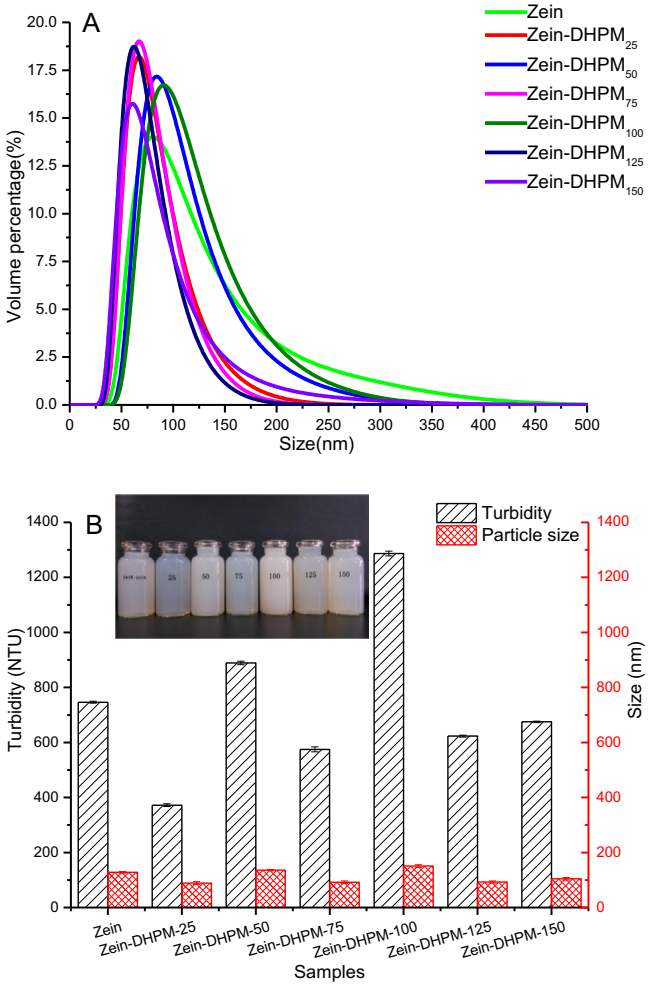

Fig. 1. Size distribution curves (A) and turbidity changes (B) of native and DHPM-treated zein colloidal dispersions.

In addition, in order to clearly reveal the relationship between the turbidity and particle size, the result of average size of native and DHPM-treated zein nanoparticles is shown in Fig. 1B. The average size of ZNP was 127.9 nm, which was obviously ($p < 0.05$) decreased to 89.1, 91.8, 92.9 and 104.8 nm for samples of Zein-DHPM$_{25}$, Zein-DHPM$_{75}$, Zein-DHPM$_{125}$ and Zein-DHPM$_{150}$, respectively. Song, Zhou, Fu, Chen, and Wu (2013) found that soy protein isolate suspension exhibited the reduction of mean particle size and narrower particle size distribution after high pressure homogenization treatment. However, the average size was significantly ($p < 0.05$) increased to 136.2 and 150.7 nm for samples of Zein-DHPM$_{50}$ and Zein-DHPM$_{100}$, respectively. It could be concluded that the change of mean particle size were consistent with that of turbidity in this work.

3.2. Fluorescence and UV spectra

Fluorescence quenching is regarded as a useful technique to provide unique information about the sensitivity of intrinsic fluorescence to the microenvironment change around proteins. The

fluorescence spectra of native and DHPM-treated zein excited at 280 nm are shown in Fig. 2 A. It can be observed that native zein exhibited a strong fluorescence emission peak at 304 nm after being excited at 280 nm. DHPM treatment at lower pressures of 25 and 50 MPa induced the decrease in relative fluorescence intensity. This result was consistent with the report from Zhang, Li, and Mittal (2010) who suggested that after high pressure processing at low pressures (<100 MPa), the relative fluorescence intensity was significantly decreased compared with that of native soybean β-conglycinin. Fluorescence quenching might be ascribed to a variety of molecular interactions including the molecular rearrangements, energy transfer, ground state complex formation and collisional quenching (Lakowicz & Masters, 2008). The decreased fluorescence intensity in this work might be attributed to the entanglement and aggregation of molecular chains, which might be generated by shear, impact and vibration at a lower treated pressure. As a result, part of the original exposed chromophores on the molecular layer was wrapped into molecular inner.

Fluorescence spectrum of the protein, when excited at 280 nm, is mainly attributed to the fluorescent emission of tryptophan residue which is sensitive to the folding and unfolding of the protein and could be applied to monitor the conformational change of the protein (Zheng & Brennan, 1998). The fluorescence intensity of zein was gradually increased upon the rise of the DHPM-treated pressure from 75 to 125 MPa, and fluorescence intensity reached to the maximum value at the pressure of 125 MPa. The increased fluorescence intensity may be ascribed to the unfolding of protein molecular chains, which were previously entangled and aggregated at a lower pressure, exposing more of the chromophores on the molecular layer due to the impact of strong shear and high-frequency vibration during the DHPM treatment. Similar results were also obtained by our previous study (Sun, Dai, Liu, & Gao, 2016). Continuously increasing the processing pressure up to 150 MPa, the fluorescence intensity of zein was slightly decreased. It may be ascribed to the fact that at a high pressure unfolded protein molecular chains were winded and aggregated again, exposing part of the chromophores entrapped in the internal molecule. These findings were consistent with the report of Wang et al. (2008) who testified that the fluorescence intensity of soy protein isolate was gradually increased with the pressure increasing from 0.1 to 600 MPa.

The tryptophan (Trp) and tyrosine (Tyr) residues are the main factors for the absorption of ultraviolet, and the absorption peak is close to the wavelength of 280 nm. From Fig. 2B, it was well known that the native zein dispersion exhibited an obvious ultraviolet absorption at 280 nm. DHPM treatment caused a significant change of the UV absorption intensity, which indicated that the structure of zein was modified. When the processing pressures were at 25 and 50 MPa, the UV absorption intensities were reduced by 5.1% and 7.3%, respectively. With the increase of treated pressure from 75 to 125 MPa, the absorption intensity was remarkably ($p < 0.05$) increased by 50.1%, which approached to the maximum. This result suggested that DHPM treatment induced part of the chromophores turning outward, exposing more tryptophan and tyrosine residues at the pressure from 75 to 125 MPa. Continuously increasing the processing pressure (150 MPa), UV absorption intensity began to decline. This result was consistent with that of the fluorescence intensity in Fig. 2A.

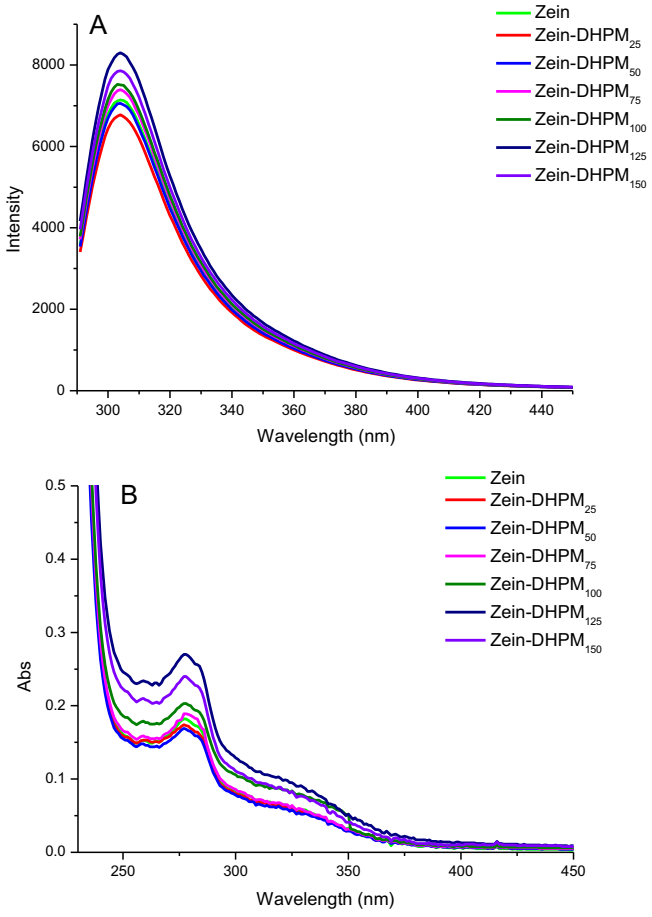

Fig. 2. Fluorescence (A) and ultraviolet absorption spectra (B) of native and DHPM-treated zein in ethanol-water solution.

3.3. CD spectra

The secondary structure of zein was evaluated using far-UV CD spectroscopy. As shown in Fig. 3, the CD spectrum of zein showed two negative peaks at 209 nm and 223 nm and a positive peak at 193 nm with a zero crossing around 202 nm, which was a characteristic of α-helical-rich secondary structure (Selling, Hamaker, & Sessa, 2007). DHPM treatment induced the secondary structure change of zein, which was reflected by the altered intensity of CD bands. The quantitative analysis of secondary structural content estimated by SELCON3 is shown in the inserted table in Fig. 3. The secondary structure composition of native zein was 57.1% α-helix, 8.6% β-sheet, 16.8% β-turn and 17.5% unordered structure, respectively. Similar result was reported by Cabra et al. (2006) who found that the range of α-helical content was 30%–60%, with the majority of the remaining structure in a random coil state. DHPM treatment at the pressure of 25 MPa led to the increase of α-helix and β-sheet from 57.1% to 59.4% and from 16.8% to 17.9%, respectively. A decrease in β-turn (from 8.6% to 5.0%) was also observed. This result may be applied to verify our hypothesis that molecular chains of zein would entangle and aggregate at lower pressures.

With the increase of processing pressure, there was a decrease in α-helix (from 57.1% to 42.6%), and an increase in random coil (from 17.5% to 33.6%), which might be ascribed to the unfolding of zein molecular chains induced by the cavitation, shear, high-velocity impact and high-frequency vibration during the DHPM treatment. Similar changing trend was also found by Zhong et al. (2014) who reported that DHPM treatment of β-lactoglobulin led to a decrease in α-helix content.

3.4. DSC

The effect of DHPM treatment on the thermal behavior of zein nanoparticles is presented in Fig. 4 and the values derived from thermal analysis are summarized in Table 1. As shown in Fig. 4A, the denaturation peak temperature (T_d) and enthalpy ($\triangle H_d$) of

Samples	Secondary structure composition (%)			
	α-helix	β-sheet	β-turn	unordered coil
Zein	57.1±0.1^{a}	8.6±0.1^{a}	16.8±0.3^{a}	17.5±0.2^{a}
Zein-DHPM$_{25}$	59.4±0.2^{b}	5.0±0.3^{b}	17.9±0.4^{a}	17.7±0.2^{a}
Zein-DHPM$_{50}$	46.8±0.1^{c}	12.9±0.2^{c}	13.4±0.2^{b}	26.9±0.3^{b}
Zein-DHPM$_{75}$	45.4±0.1^{c}	11.8±0.2^{c}	12.6±0.2^{b}	30.2±0.4^{b}
Zein-DHPM$_{100}$	49.0±0.2^{d}	7.5±0.3^{d}	14.0±0.3^{b}	29.5±0.3^{b}
Zein-DHPM$_{125}$	45.4±0.1^{c}	10.7±0.1^{c}	14.2±0.3^{b}	29.8±0.2^{b}
Zein-DHPM$_{150}$	42.6±0.1^{e}	12.1±0.2^{c}	11.7±0.2^{b}	33.6±0.5^{c}

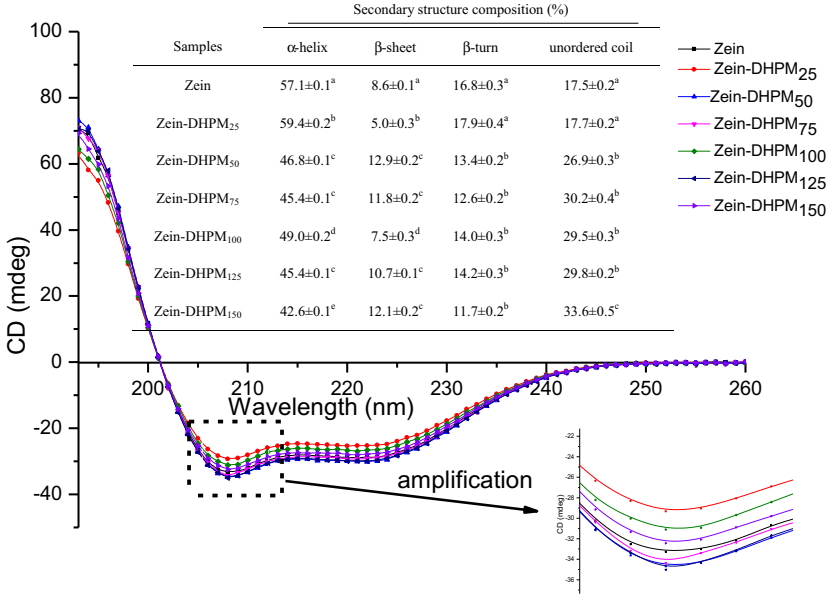

Fig. 3. CD spectra of native and DHPM-treated zein in ethanol-water solution. As shown from the inserted table, values are means ± standard deviation of triplicate analyses and different superscript letters in the same column indicate significant differences ($p < 0.05$).

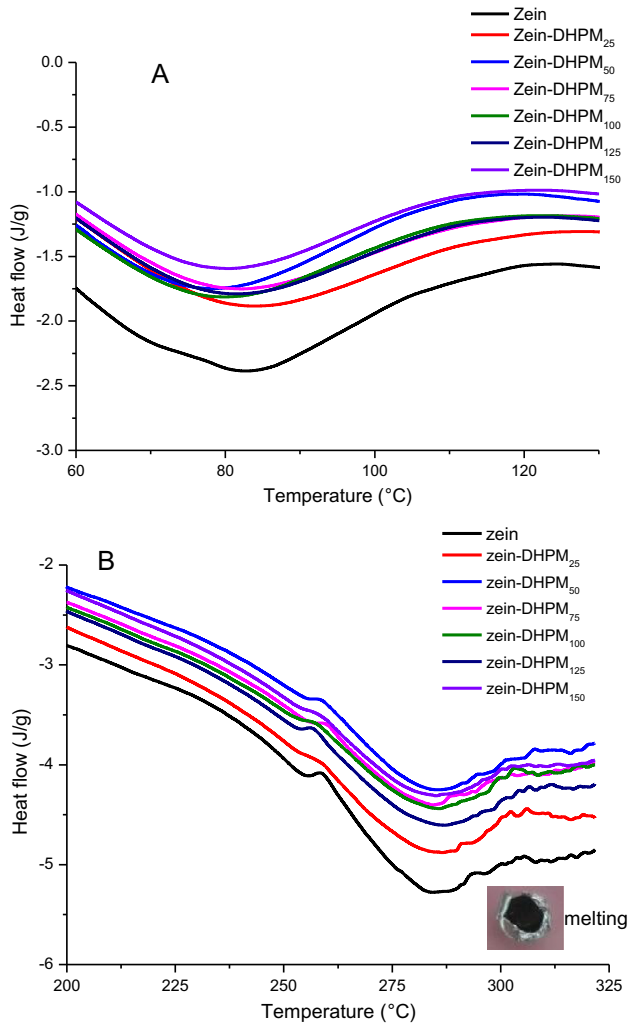

Fig. 4. DSC thermograms of native and DHPM-treated zein colloidal nanoparticles. A: denatured curves; B: melting curves.

Table 1
Effect of DHPM treatment on the thermal behaviors of zein nanoparticles.

Samples	T_d (°C)	$\triangle H_d$ (J/g)	T_m (°C)	$\triangle H_m$ (J/g)
Zein	82.6 ± 0.3^{a}	−83.4 ± 2.7^{a}	284.4 ± 0.1^{a}	−102.5 ± 3.1^{a}
Zein-DHPM$_{25}$	83.5 ± 0.1^{b}	−59.7 ± 3.6^{b}	286.6 ± 0.3^{b}	−56.8 ± 2.3^{b}
Zein-DHPM$_{50}$	78.2 ± 0.1^{c}	−51.4 ± 1.2^{c}	285.8 ± 0.1^{c}	−68.9 ± 1.8^{c}
Zein-DHPM$_{75}$	82.0 ± 0.2^{a}	−60.4 ± 2.1^{b}	284.3 ± 0.2^{a}	−63.1 ± 1.5^{d}
Zein-DHPM$_{100}$	80.0 ± 0.1^{d}	−53.0 ± 0.8^{c}	285.6 ± 0.3^{c}	−63.4 ± 2.0^{b}
Zein-DHPM$_{125}$	81.3 ± 0.2^{a}	−54.3 ± 1.0^{d}	287.1 ± 0.2^{b}	−66.8 ± 1.9^{c}
Zein-DHPM$_{150}$	80.5 ± 0.2^{d}	−58.4 ± 2.2^{b}	285.2 ± 0.4^{c}	−72.4 ± 1.2^{e}

T_d: denaturation temperature; $\triangle H_d$: denaturation enthalpy; T_m: melting temperature; $\triangle H_m$: melting enthalpy. Values are means ± standard deviation of triplicate analyses. Different superscript letters in the same column indicate significant differences ($p < 0.05$).

native zein nanoparticles was 82.6 °C and −83.4 J/g, respectively. DHPM treatment at the pressure of 25 MPa led to a slight increase of T_d to 83.5 °C. The increased T_d might be attributed to the fact that zein molecular chains were partially folded, which was induced by DHPM treatment at a low pressure and it could be also confirmed by the narrower size distribution as shown in Fig. 1A. Keerati-u-rai and Corredig (2009) found that an increase of the thermal transition peak temperature was observed in the soy protein isolate, as the peak temperature was increased from 68.3 to 69.2 °C after treated at the high pressure (65 MPa).

With the increase of processing pressure, DHPM treatment resulted in the decrease of denaturation temperature and enthalpy, which implied that DHPM treatment induced the partial denaturation of zein. This result might be due to the occurrence of the unfolding behavior of zein molecular chains induced by DHPM treatment at high pressures. Floury, Desrumaux, and Legrand (2002) observed a similar behavior after soy proteins were treated by ultra high pressure homogenization treatment. Hayakawa, Linko, and Linko (1996) pointed out that the high mechanical forces during high pressure dynamic homogenization induced the structural rearrangements of protein molecules. Moreover, it was worth mentioning that the thermal behavior of zein nanoparticles was dependent on the treated pressure levels during the DHPM treatment.

Fig. 4B indicates the melting process of zein with the rise of temperature after thermal denaturation, and the melting phe-

nomenon can be directly observed. As shown in Table 1, the melting temperature (T_m) and enthalpy ($\triangle H_m$) of native zein nanoparticles were 284.4 °C and −102.5 J/g, respectively. After DHPM treatment, the T_m of zein nanoparticles was slightly increased to 287.1 °C. However, $\triangle H_m$ exhibited a significant ($p < 0.05$) decrease to −56.8 J/g, which further confirmed the denaturation of zein due to the DHPM treatment.

3.5. TEM

The microstructure of the samples was observed by transmission electron microscopy to evaluate the effect of DHPM treatment on the morphological characteristics of zein nanoparticles. As shown in Fig. 5, native zein nanoparticle (Fig. 5A) exhibited a typical shape of nanosphere, which was consistent with the findings of

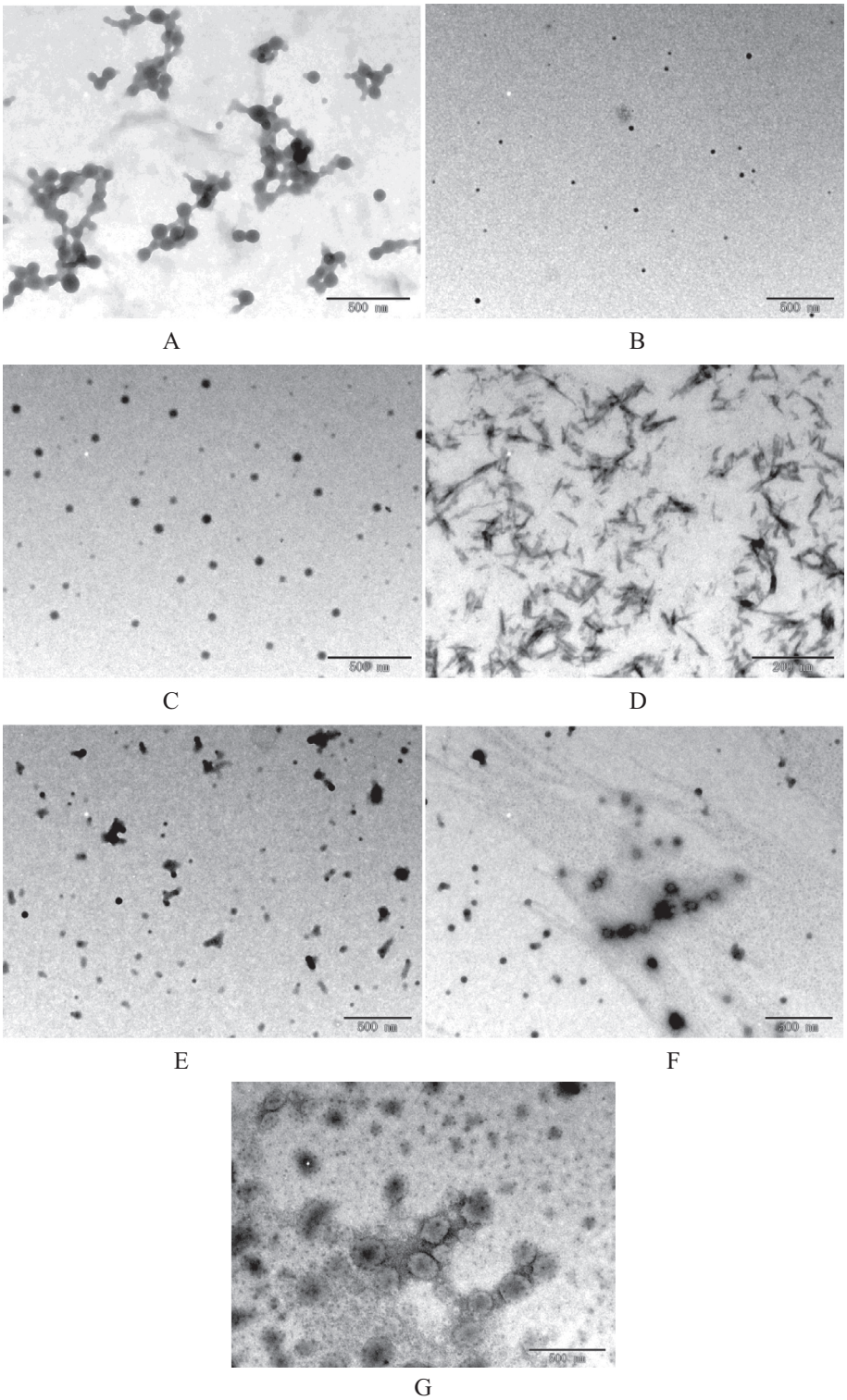

Fig. 5. TEM images of native and DHPM-treated zein colloidal nanoparticles. A: Zein; B: Zein-$DHPM_{25}$; C: Zein-$DHPM_{50}$; D: Zein-$DHPM_{75}$; E: Zein-$DHPM_{100}$; F: Zein-$DHPM_{125}$; G: Zein-$DHPM_{150}$.

Wu, Luo, and Wang (2012). However, the phenomenon of adhesion among the native zein nanoparticles was observed and the particle distribution was inhomogeneous. After DHPM treatment at the pressures of 25 (Fig. 5B) and 50 MPa (Fig. 5C), zein nanoparticles remained the original morphology of nanosphere but showed a notably reduced size with a monodisperse distribution, which was consistent with the findings of O'Sullivan, Murray, Flynn, and Norton (2015) who reported that ultrasound treatment of soy protein isolate induced the disruption of protein aggregates.

However, after DHPM treatment at 75 MPa, the morphology of zein was changed from the original sphere to the needle-like and linear shape (Fig. 5D). Hu, Zhao, Sun, Zhao, and Ren (2011) reported that fragmentized clumps of peanut protein isolate were generated in different sizes and shapes by DHPM treatment. Besides, the discrete spheroids and random geometric entities were also observed when the treatment pressure reached to 100 MPa (Fig. 5E). To explain these findings, the deduction was put forward in present work that the morphological change of zein particles at 75 MPa was ascribed to the existence of the intermediate transition state and the pressure of 75 MPa was estimated to be a critical value of the morphological transformation. Zein particles were maintained in the original state when the processing pressure (less than 75 MPa) was not enough to regulate the structure of zein. However, when the processing pressure was more than 75 MPa, linear molecules were reaggregated to form the irregular shape and part of the aggregates was transformed into spherical particles.

As the processing pressure was continuously increased (125 MPa), spherical particles and part of the smaller particles with the core-shell structure occurred as shown in Fig. 5F. When the pressure reached to 150 MPa, larger particles with obvious core-shell structure were observed as shown in Fig. 5G. This might be because higher pressure enhanced the contact frequency of the particles, which resulted in the aggregation of smaller particles and the formation of larger particles. Previous studies interpreted that new disulfide bonds and the exposition of hydrophobic sites could lead to the aggregation after the pressure-induced dissociation (Zhang, Li, Tatsumi, & Isobe, 2005).

4. Conclusions

The changes of physical and structural properties of zein induced by DHPM treatment were mainly associated with the special processing pressure, which presented certain regularity at an interval of 50 MPa. According to the analysis of the microstructure of the samples, the deduction was proposed that the morphological change of zein particles at 75 MPa was ascribed to the existence of the intermediate transition state. The DHPM modification technology might be an attractive method to develop new food biopolymers with better thermal behaviors and structural properties, which could be useful in the development of the delivery systems for bioactive compounds.

Acknowledgement

Financial support from the National Natural Science Foundation of China (No. 31371835) is gratefully acknowledged.

References

Argos, P., Pedersen, K., Marks, M. D., & Larkins, B. A. (1982). A structural model for maize zein proteins. *Journal of Biological Chemistry, 257*(17), 9984–9990.

Arzeni, C., Martinez, K., Zema, P., Arias, A., Perez, O. E., & Pilosof, A. M. R. (2012). Comparative study of high intensity ultrasound effects on food proteins functionality. *Journal of Food Engineering, 108*(3), 463–472.

Cabra, V., Arreguin, R., Vazquez-Duhalt, R., & Farres, A. (2006). Effect of temperature and pH on the secondary structure and processes of oligomerization of 19 kDa alpha-zein. *Biochimica et Biophysica Acta (BBA) – Proteins and Proteomics, 1764*(6), 1110–1118.

Chen, J., Gao, D., Yang, L., & Gao, Y. (2013). Effect of microfluidization process on the functional properties of insoluble dietary fiber. *Food Research International, 54*(2), 1821–1827.

Ciron, C. I. E., Gee, V. L., Kelly, A. L., & Auty, M. A. E. (2010). Comparison of the effects of high-pressure microfluidization and conventional homogenization of milk on particle size, water retention and texture of non-fat and low-fat yoghurts. *International Dairy Journal, 20*(5), 314–320.

Cook, E. J., & Lagace, A. P. (1987). Forming a microemulsion-comprises impinging streams of mixtures containing components of micro-emulsion into each other at high pressure in low pressure zone. *US Patent*. US4908154-A.

Floury, J., Desrumaux, A., & Legrand, J. (2002). Effect of ultra-high pressure homogenization on structure and on rheological properties of soy protein stabilized emulsions. *Journal of Food Science, 67*, 3388–3395.

Funatsu, G., & Shibata, M. (1998). Modified zein and its production. *Patent JP*. 10017595.

Hayakawa, I., Linko, Y. Y., & Linko, P. (1996). Mechanism of high pressure denaturation of proteins. *LWT – Food Science and Technology, 29*(8), 756–762.

Hayes, M. G., Fox, P. F., & Kelly, A. L. (2005). Potential applications of high pressure homogenisation in processing of liquid milk. *Journal of Dairy Research, 72*(01), 25–33.

Hu, X., Zhao, M., Sun, W., Zhao, G., & Ren, J. (2011). Effects of microfluidization treatment and transglutaminase cross-linking on physicochemical, functional, and conformational properties of peanut protein isolate. *Journal of Agricultural and Food Chemistry, 59*(16), 8886–8894.

Keerati-u-rai, M., & Corredig, M. (2009). Effect of dynamic high pressure homogenization on the aggregation state of soy protein. *Journal of Agricultural and Food Chemistry, 57*(9), 3556–3562.

Lajunen, T., Hisazumi, K., Kanazawa, T., Okada, H., Seta, Y., Yliperttula, M., Urtti, A., et al. (2014). Topical drug delivery to retinal pigment epithelium with microfluidizer produced small liposomes. *European Journal of Pharmaceutical Sciences, 62*, 23–32.

Lakowicz, J. R., & Masters, B. R. (2008). Principles of fluorescence spectroscopy. *Journal of Biomedical Optics, 13*(2), 9901.

Lawton, J. W. (2002). Zein: A history of processing and use. *Cereal Chemistry, 79*(1), 1–18.

Lobley, A., Whitmore, L., & Wallace, B. A. (2002). DICHROWEB: An interactive website for the analysis of protein secondary structure from circular dichroism spectra. *Bioinformatics, 18*(1), 211–212.

Luo, Y., Teng, Z., Wang, T. T., & Wang, Q. (2013). Cellular uptake and transport of zein nanoparticles: effects of sodium caseinate. *Journal of Agricultural and Food Chemistry, 61*(31), 7621–7629.

Matsushima, N., Danno, G. I., Takezawa, H., & Izumi, Y. (1997). Three-dimensional structure of maize α-zein proteins studied by small-angle X-ray scattering. *Biochimica et Biophysica Acta – Protein Structure and Molecular Enzymology, 1339*(1), 14–22.

Mizutani, Y., Matsumura, Y., Murakami, H., & Mori, T. (2004). Effects of heating on the interaction of lipid and zein in a dry powder system. *Journal of Agricultural and Food Chemistry, 52*(11), 3570–3576.

Osborne, T. B. (1897). The amount and properties of the proteids of the maize kernel. *Journal of the American Chemical Society, 19*(7), 525–532.

O'Sullivan, J., Murray, B., Flynn, C., & Norton, I. (2015). The effect of ultrasound treatment on the structural, physical and emulsifying properties of animal and vegetable proteins. *Food Hydrocolloids, 53*, 141–154.

Paliwal, R., & Palakurthi, S. (2014). Zein in controlled drug delivery and tissue engineering. *Journal of Controlled Release, 189*, 108–122.

Patel, A. R., Bouwens, E. C., & Velikov, K. P. (2010). Sodium caseinate stabilized zein colloidal particles. *Journal of Agricultural and Food Chemistry, 58*(23), 12497–12503.

Patel, A. R., & Velikov, K. P. (2014). Zein as a source of functional colloidal nano-and microstructures. *Current Opinion in Colloid & Interface Science, 19*(5), 450–458.

Pereda, J., Ferragut, V., Quevedo, J. M., Guamis, B., & Trujillo, A. J. (2008). Effects of ultra-high-pressure homogenization treatment on the lipolysis and lipid oxidation of milk during refrigerated storage. *Journal of Agricultural and Food Chemistry, 56*(16), 7125–7130.

Selling, G. W., Hamaker, S. A., & Sessa, D. J. (2007). Effect of solvent and temperature on secondary and tertiary structure of zein by circular dichroism. *Cereal Chemistry, 84*(3), 265–270.

Shen, L., & Tang, C. H. (2012). Microfluidization as a potential technique to modify surface properties of soy protein isolate. *Food Research International, 48*(1), 108–118.

Song, X., Zhou, C., Fu, F., Chen, Z., & Wu, Q. (2013). Effect of high-pressure homogenization on particle size and film properties of soy protein isolate. *Industrial Crops and Products, 43*, 538–544.

Sun, C., Dai, L., Liu, F., & Gao, Y. (2016). Simultaneous treatment of heat and high pressure homogenization of zein in ethanol-water solution: Physical, structural, thermal and morphological characteristics. *Innovative Food Science & Emerging Technologies, 34*, 161–170.

Sun, C., Liu, F., Yang, J., Yang, W., Yuan, F., & Gao, Y. (2015). Physical, structural, thermal and morphological characteristics of zein-quercetagetin composite colloidal nanoparticles. *Industrial Crops and Products, 77*, 476–483.

Wang, L. J., Hu, Y. Q., Yin, S. W., Yang, X. Q., Lai, F. R., & Wang, S. Q. (2015). Fabrication and characterization of antioxidant pickering emulsions stabilized by zein/chitosan complex particles. *Journal of Agricultural and Food Chemistry, 63*(9), 2514–2524.

Wang, X. S., Tang, C. H., Li, B. S., Yang, X. Q., Li, L., & Ma, C. Y. (2008). Effects of high-pressure treatment on some physicochemical and functional properties of soy protein isolates. *Food Hydrocolloids, 22*(4), 560–567.

Wu, Y., Luo, Y., & Wang, Q. (2012). Antioxidant and antimicrobial properties of essential oils encapsulated in zein nanoparticles prepared by liquid-liquid dispersion method. *LWT – Food Science and Technology, 48*(2), 283–290.

Yamada, K., Noguchi, A., & Takhashi, H. (1996). Effects of solvents on properties of zein. *Nippon Shokuhin Kogaku Kaishi, 43*, 306–312.

Zhang, H., Li, L., & Mittal, G. S. (2010). Effects of high pressure processing on soybean beta-conglycinin. *Journal of Food Process Engineering, 33*(3), 568–583.

Zhang, H., Li, L., Tatsumi, E., & Isobe, S. (2005). High-pressure treatment effects on proteins in soy milk. *LWT – Food Science and Technology, 38*(1), 7–14.

Zheng, L., & Brennan, J. D. (1998). Measurement of intrinsic fluorescence to probe the conformational flexibility and thermodynamic stability of a single tryptophan protein entrapped in a sol–gel derived glass matrix. *Analyst, 123*(8), 1735–1744.

Zhong, J., Tu, Y., Liu, W., Xu, Y., Liu, C., & Dun, R. (2014). Antigenicity and conformational changes of β-lactoglobulin by dynamic high pressure microfluidization combining with glycation treatment. *Journal of Dairy Science, 97*(8), 4695–4702.